

Metal-Assisted and Solvent-Mediated Synthesis of Two-Dimensional Triazine Structures on Gram Scale

Abbas Faghani, Mohammad Fardin Gholami, Matthias Trunk, Johannes Müller, Pradip Pachfule, Sarah Vogl, Ievgen Donskyi, Philip Nickl, Jingjing Shao, Michael R.S. Huang, Wolfgang E. S. Unger, Raul Arenal, Christoph T. Koch, Beate Paulus, Jürgen P. Rabe, Arne Thomas, Rainer Haag, and Mohsen Adeli

J. Am. Chem. Soc., **Just Accepted Manuscript** • DOI: 10.1021/jacs.0c02399 • Publication Date (Web): 27 Jun 2020

Downloaded from pubs.acs.org on June 27, 2020

Just Accepted

“Just Accepted” manuscripts have been peer-reviewed and accepted for publication. They are posted online prior to technical editing, formatting for publication and author proofing. The American Chemical Society provides “Just Accepted” as a service to the research community to expedite the dissemination of scientific material as soon as possible after acceptance. “Just Accepted” manuscripts appear in full in PDF format accompanied by an HTML abstract. “Just Accepted” manuscripts have been fully peer reviewed, but should not be considered the official version of record. They are citable by the Digital Object Identifier (DOI®). “Just Accepted” is an optional service offered to authors. Therefore, the “Just Accepted” Web site may not include all articles that will be published in the journal. After a manuscript is technically edited and formatted, it will be removed from the “Just Accepted” Web site and published as an ASAP article. Note that technical editing may introduce minor changes to the manuscript text and/or graphics which could affect content, and all legal disclaimers and ethical guidelines that apply to the journal pertain. ACS cannot be held responsible for errors or consequences arising from the use of information contained in these “Just Accepted” manuscripts.

Metal-Assisted and Solvent-Mediated Synthesis of Two-Dimensional Triazine Structures on Gram Scale

Abbas Faghani, Mohammad Fardin Gholami, Matthias Trunk, Johannes Müller, Pradip Pachfule, Sarah Vogl, Ievgen Donskyi, Mingjun Li, Philip Nickl, Jingjing Shao, Michael Huang, Wolfgang E. S. Unger, Raul Arenal, Christoph T. Koch, Beate Paulus, Jürgen P. Rabe, Arne Thomas, Rainer Haag and Mohsen Adeli**

ABSTRACT: Covalent triazine frameworks are an emerging material class, which have shown promising performance for a range of applications. In this work, we report on a metal-assisted and solvent-mediated reaction between calcium carbide and cyanuric chloride, as cheap and commercially available precursors, to synthesize two-dimensional triazine structures (2DTSs). The reaction between dimethylformamide and cyanuric chloride was promoted by calcium carbide and resulted in dimethylamino-*s*-triazine intermediates which in turn undergo nucleophilic substitutions. This reaction was directed into two dimensions by calcium ions derived from calcium carbide and induced the formation of 2DTSs. The role of calcium ions to direct the two-dimensionality of the final structure was simulated using DFT and further proven by synthesizing molecular intermediates. The water content of the reaction medium was found to be a crucial factor that affected the structure of the products dramatically. While 2DTSs were obtained at anhydrous conditions, a mixture of graphitic material/2DTSs or only graphitic material (GM) was obtained in aqueous solutions. Taking advantage of the straightforward and gram-scale synthesis of 2DTSs, as well as their photothermal and photodynamic properties, they are promising materials for a wide range of future applications including bacteria and virus incapacitation.

Keywords: Two-dimensional polymer, two-dimensional polymerization, calcium carbide, triazine framework

INTRODUCTION

Reticular chemistry has notably extended the scope of two and three-dimensional porous structures.¹⁻⁴ Two-dimensional polymers,⁵ metal organic frameworks,⁶ covalent organic frameworks,⁷ and polymeric networks⁸ with complex but known structures are designed and prepared by this strategy. These materials have shown a high potential for the future applications ranging from energy storage⁹ to membrane separation.¹⁰

However, two-dimensional covalent organic frameworks with versatile but defined structures are at the forefront of this rapidly developing field of chemistry.¹¹⁻¹⁴ Also, triazine-based structures with unique physicochemical properties have been intensively investigated in the last decade.¹⁵⁻¹⁹ Microporous triazine-based structures²⁰ with diverse applications in gas adsorption and storage,²¹⁻²⁵ catalysis,²⁶⁻²⁹ and energy storage³⁰⁻³² have been prepared by a variety of synthetic methods.³³ Trimerization of nitriles, for example, is a straightforward and one-pot synthetic approach by which triazine-based structures with high surface area have been prepared.¹⁶ However, most of the current synthetic methods require high reaction temperatures, which lead to partial carbonization and undefined structures.³⁴⁻³⁵ Triazine-based structures²⁰ synthesized by such methods do not show an electronic band gap and useful optoelectronic properties, due to side reactions at high temperatures.³⁵ Therefore, it is crucial to develop new strategies to synthesize more defined structures with useful optical and electronic properties.³² Recently, the synthesis of triazine-based structures has been improved using acid-catalyzed microwave³⁶ and mechano-chemistry,³⁷ which elaborate the current harsh synthetic conditions of ionothermal trimerization. However, the synthesis of triazine structures in solution, through which kinetic and thermodynamic parameters of reactions could be manipulated, has not been considerably developed. The lack of efficient synthetic methods in solution is a problem that has limited the structural diversity of triazine-based structures and hampered their practical usage.¹⁹ In addition to synthetic challenges, the preparation of triazine-based structures in mono- and few-layered forms is another problem for attaining unique characteristics of two-dimensional nanomaterials.^{28, 38-39} This objection affects the efficiency of these materials, where thickness and number of layers play a significant role.

Recently, triazine-based structures have been synthesized by a polycondensation reaction of aldehydes and amidines at relatively mild conditions.^{15, 35} Although frameworks synthesized by this method have shown layered structures, superior to previous works, they could not be found in mono-layer form.³⁹ Stacking of covalent triazine-based structures in multi-layered structures diminishes their accessible surface area and changes their

1
2
3 physicochemical properties. Aldehyde-amidine polycondensation is a straightforward reaction
4 for gram-scale synthesis of triazine-based structures but is limited by availability of the
5 synthetic monomers. Furthermore, purification of triazine based structures is a time-
6 consuming process and requires washing at relatively high temperatures.⁴⁰ This process is not
7 compatible with reactive functional groups and less stable frameworks. Very recently,
8 triazine-based olefin-linked structures⁴¹ have been reported, where triazine units can be
9 stitched on to other organic linkers via covalent bonding.⁴² Although, these fully conjugated
10 and crystalline triazine-based structures have shown interesting properties, this research topic
11 is still in its infancy and need more attention for bringing out a general synthesis protocol for
12 various structures in bulk-scale. Accordingly, scale-up, cost-efficiency, purification process,
13 reaction parameters, and environmental aspects of classical synthetic methods require to be
14 improved to economically obtain covalent mono-layer triazine frameworks with desired
15 physicochemical properties.

16
17 In this work, we have addressed these challenges by metal-assisted and solvent-
18 mediated synthesis of two-dimensional triazine structures (2DTSs). Reaction between calcium
19 carbide and cyanuric chloride in dimethylformamide (DMF) resulted in 2DTSs with several
20 micrometer lateral sizes. While cyanuric chloride acts as the source of triazine units, calcium
21 carbide provides both acetylide linkages and calcium ions. The reaction was mediated by
22 DMF and directed in two dimensions by calcium ions, leading to 2DTSs after trimerization of
23 triple bonds. Adding water to the reaction medium changed the structure of the product from
24 2DTSs, in anhydrous conditions, to graphitic materials. Taking advantage of the π -conjugated
25 system of their triazine backbone, 2DTSs can be developed for future applications such as
26 photocatalysis,⁴³ electrocatalysis,⁴⁴ supercapacitors³² and Li-ion battery.⁴⁵ However, in this
27 manuscript, we have focused on the synthesis and physicochemical properties of 2DTSs, in
28 addition to their mechanistic investigations.

29 30 31 32 33 34 35 36 37 38 39 40 41 42 43 44 45 46 47 48 **RESULTS AND DISCUSSION**

49 The reaction between cyanuric chloride and DMF at different conditions results in versatile
50 intermediates.⁴⁶⁻⁴⁸ Herein, we demonstrate that this reaction, in the presence of calcium
51 carbide, yields 2-(*N,N*-dimethylamino)-4,6-dichloro-*s*-triazine, which undergoes consecutive
52 nucleophilic aromatic substitutions by acetylide dianions and produces two-dimensional
53 triazine structures after trimerization (Figure 1). Calcium ions directed the carbon-carbon
54 coupling of monomers in two dimensions and were eventually removed by washing (see page
55
56
57
58
59
60

1
2
3 S7). This reaction was performed under different conditions and the effect of water content on
4 the structure of the products was monitored (Figure 1).
5

6 In order to carry out reactions, calcium carbide and cyanuric chloride were mixed and
7 stirred in bulk under inert atmosphere and then dispersed in DMF. Depending on the amount
8 of water present during the reaction, the product varied from crystalline graphitic material to
9 pure 2DTSs (Figure 1). The structures of the products were analyzed by different
10 spectroscopy and microscopy methods as well as elemental and thermal analysis. Also, the
11 reaction mechanisms were investigated by synthesizing different model compounds and
12 studying the structure of intermediates (*vide infra*).
13
14
15
16
17
18

19 High resolution transmission electron microscopy (HRTEM) and scanning electron
20 microscopy (SEM) images revealed the formation of layered and bulk structures with lateral
21 sizes of several micrometers for the products of reactions at different conditions (Figures
22 2a,b,d,e). Further investigations revealed that water affected the structure of the reaction
23 products dramatically. The product of the reaction between calcium carbide and water was
24 crystalline with a measured in-plane lattice constant of the hexagonal crystal of approximately
25 0.248 nm (min: 0.241 nm, max: 0.254 nm, see Figure S1). This corresponds well to the in-
26 plane lattice constant of graphite ($a = 0.246$ nm). These results were consistently obtained by
27 HRTEM imaging and electron diffraction in the SEM. Furthermore, EDX elemental analysis
28 of the crystalline particles concluded approximately 99% carbon, which indicates, together
29 with the hexagonal unit cell, that the material is graphite. In anhydrous conditions (see page
30 S7), however, a product with an amorphous structure was obtained (Figure 2c, Figure S4),
31 which we determined to be 2DTSs. Electron energy loss spectroscopy (EELS) spectra showed
32 discrete peaks at ~ 285 eV and ~ 400 eV, which were assigned to carbon and nitrogen in the
33 backbone of this material (Figure S3).⁴⁹⁻⁵²
34
35
36
37
38
39
40
41
42
43
44
45
46
47
48
49
50
51
52
53
54
55
56
57
58
59
60

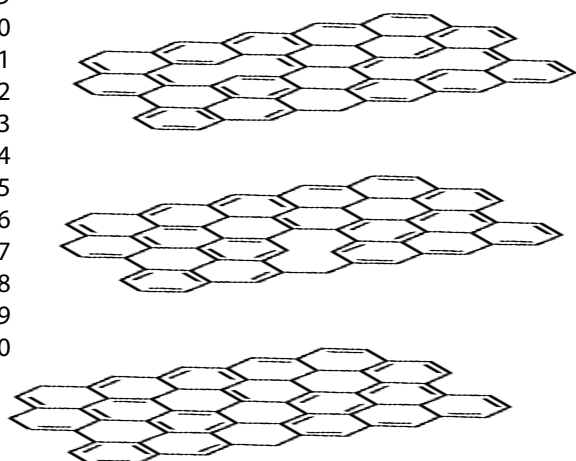
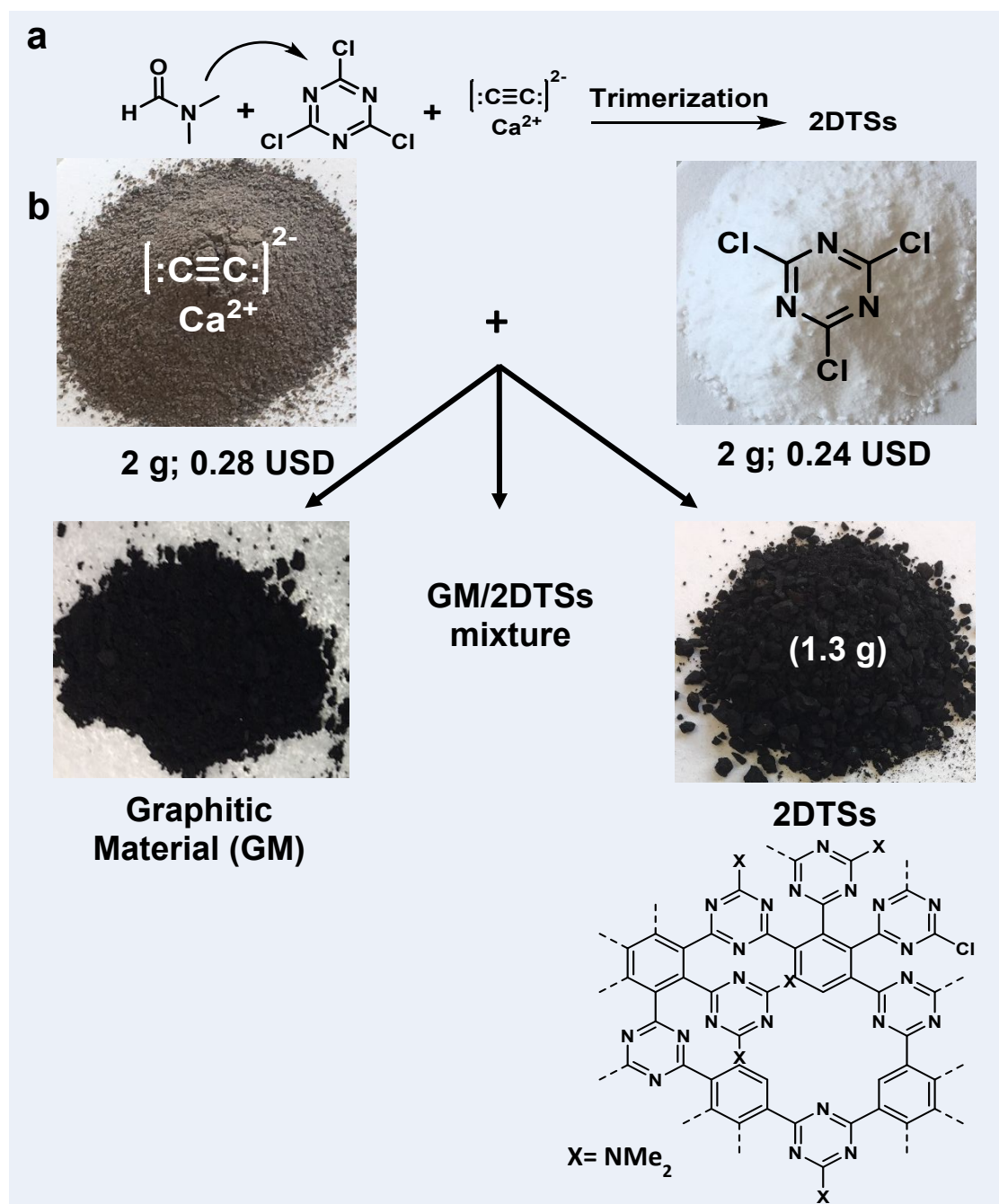


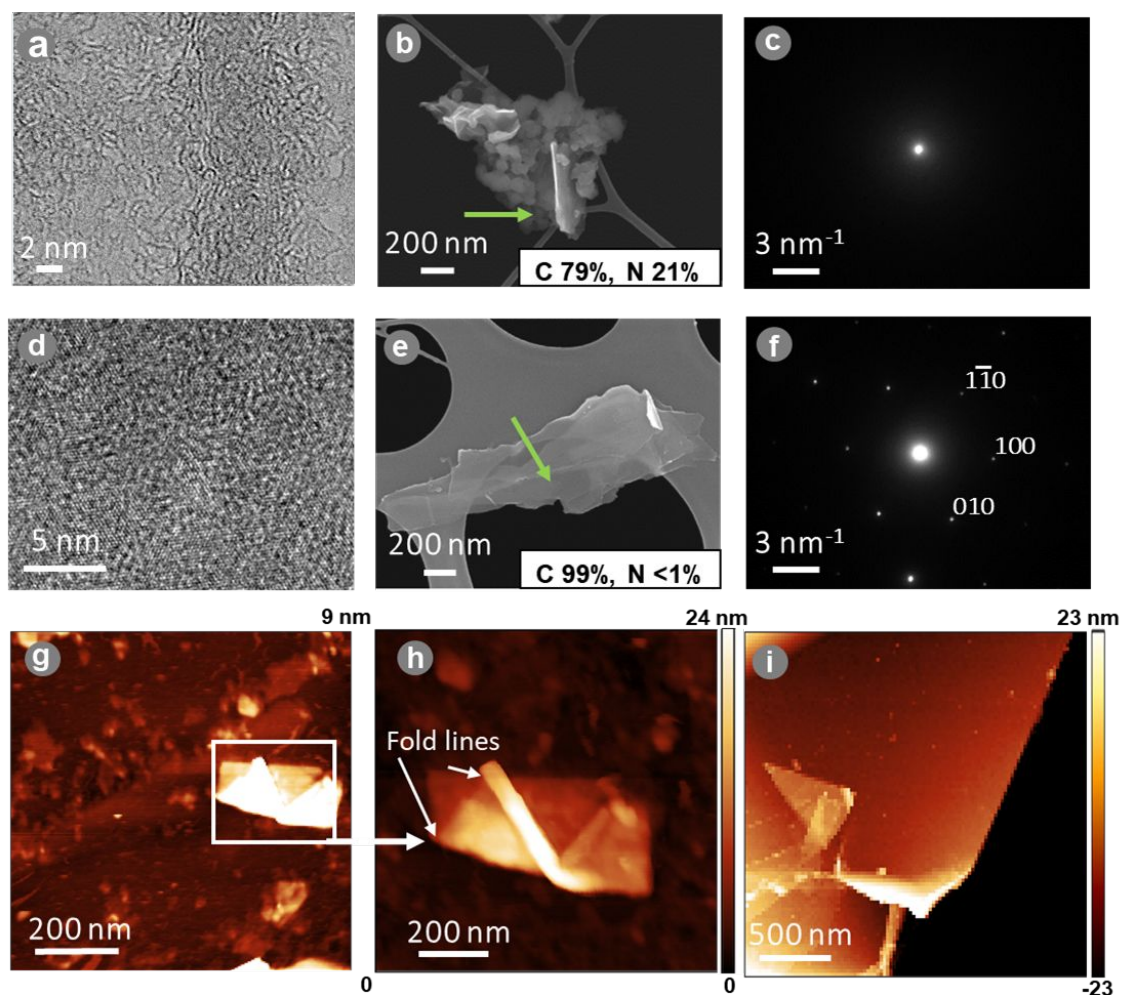
Figure 1. (a) Reaction between triazine and calcium carbide in anhydrous DMF resulted in

1
2
3 2DTSS. (b) The product of the reaction between calcium carbide and triazine was strongly
4 influenced by the water content of the solvent. While graphitic material (GM) was the main
5 product in aqueous solutions (water, 25 °C, 30 minutes), 2DTSSs were obtained in anhydrous
6 DMF (120 °C, 72 hours). Also, a mixture of GM/2DTSSs was created in non-anhydrous DMF
7 (120 °C, 72 hours). The cost-effectiveness of the reaction is shown by the estimated prices
8 and quantities of the precursors. Prices of reagents were monitored from commercial suppliers
9 (see page S3).
10
11
12
13
14
15
16

17 The nitrogen content of the reaction products at different conditions, which is an
18 indicator for the triazine rings, was further investigated by elemental analysis. While the
19 nitrogen content of the reaction product in water (GM) was close to zero, it increased to ~21%
20 for the product of reaction under anhydrous conditions (Table S1). Under anhydrous
21 conditions the carbon/nitrogen ratio of the product was 2.6, yielding approximately a C₃N₁
22 molecular formula for 2DTSSs (Table S1). This carbon/nitrogen ratio indicated the formation
23 of graphitic domains⁵³⁻⁵⁴ in 2DTSSs by acetylide cross-coupling and trimerization (Figure 3d).
24
25
26
27
28

29 The topography and size of the product of reaction under anhydrous condition was
30 further investigated by scanning force microscopy in quantitative nanomechanical mapping
31 mode (SFM-QNM) on a freshly cleaved mica surface (Figures 2g,h and Figures S5a,b). It
32 revealed layered structures with lateral sizes of 2 to 3 micrometers and thicknesses of 100 to
33 350 nm, with layers and terraces including smaller layers with self-overlapping regions (folds)
34 and an inhomogeneous distribution of mobile and small interconnected particles above the
35 larger flakes, with a RMS roughness of 1 nm. Since the heights of the layers were between 5
36 to 10 nm, we believe that we did not observe a single-layer exfoliation of the layered
37 structures. However, exfoliated multilayered structures exhibited self-avoiding behavior as
38 evident in back folding,⁵⁵⁻⁵⁶ which may be simulated on macroscale using a sheet of paper for
39 Figure 2h (Figure S5c). Self-avoidance of a structure is a direct consequence of its covalent
40 bonding within a 2D network. This is indeed not the case for self-assembled 2D structures
41 such as lipid bilayers/membranes, as those structures can self-penetrate and restructure back
42 to a single layer rather than stabilize in a folded conformation. An observation of folding in
43 case of 2D covalent structures is possible only when there is an overall gain in the energy of
44 the system. This can be achieved by van der Waals interlayer forces (similar to those present
45 within layers of a crystal) triggered by drying process during surface deposition.⁵⁶ The
46 product of the reaction between calcium carbide and cyanuric chloride in DMF under ambient
47 condition (Figure 1, midline), which is called 2DTSSs/GM, was also investigated by different
48
49
50
51
52
53
54
55
56
57
58
59
60

1
2
3 characterization methods including TEM, EDX, elemental and thermal analysis. It was found
4 that this product is always a mixture of 2DTSs and graphitic material (Table S1, Figure 3b).
5 Attenuated total reflection infrared spectroscopy (ATR-FTIR) of 2DTSs revealed a broad
6 absorbance band at $\sim 1394\text{-}1577\text{ cm}^{-1}$ that corresponds to carbon-carbon and carbon-nitrogen
7 double bonds. The absence of the triple-bond absorbance and the appearance of C=C
8 vibrations in the IR spectrum of 2DTSs are attributed to the trimerization of triple bonds and
9 the formation of benzene rings (Figure S6). Also, an absorbance band at 3300 cm^{-1} indicated
10 presence of hydroxyl functional groups in the structure of 2DTSs, which have been created by
11 the reaction between unreacted chlorine atoms of cyanuric chloride and water in the
12 purification process.
13
14
15
16
17
18
19
20
21
22



54 **Figure 2.** The products were investigated by different microscopy methods including
55 HRTEM, SEM and SFM. (a) and (d) HRTEM images of 2DTSs and GM, respectively. (b)
56 and (e) SEM images of 2DTSs and graphitic material on top of holey carbon TEM grids,
57 respectively. (Insets are carbon and nitrogen contents of the indicated area obtained by
58 energy-dispersive X-ray spectroscopy (EDX).) (c) and (f) Diffraction patterns of 2DTSs and
59
60

1
2
3 GM at the indicated areas of **(b)** and **(e)** that show amorphous and crystalline characteristics
4 for these materials, respectively. The in-plane unit cell parameter of the hexagonal lattice of
5 GM was on average 0.248 nm. **(g)** SFM-QNM height image of the product of reaction in
6 anhydrous condition with plateaus and terraces (more images in Figure S5), **(h)** A close-up
7 image of a sheet obtained in anhydrous condition with back folding. Planar layer topography
8 is evident from the height image. **(i)** SFM-QNM height images of a large plateau of graphitic
9 material.
10
11
12
13
14
15
16

17 ^{13}C solid-state cross-polarization-magic-angle-spinning (CP-MAS) nuclear magnetic
18 resonance (NMR) spectra of 2DTS showed a broad signal at 148-162 ppm, which is assigned
19 to the carbon atoms of triazine rings⁵⁷⁻⁵⁸ and a signal at 27 ppm for $-\text{NMe}_2$ groups (Figure 3a).
20 In this spectrum, a broad signal centered at 126 ppm is assigned to benzene rings, which is a
21 further proof for the trimerization of triple bonds (Figure 3a).
22
23
24
25
26
27
28
29
30
31
32
33
34
35
36
37
38
39
40
41
42
43
44
45
46
47
48
49
50
51
52
53
54
55
56
57
58
59
60

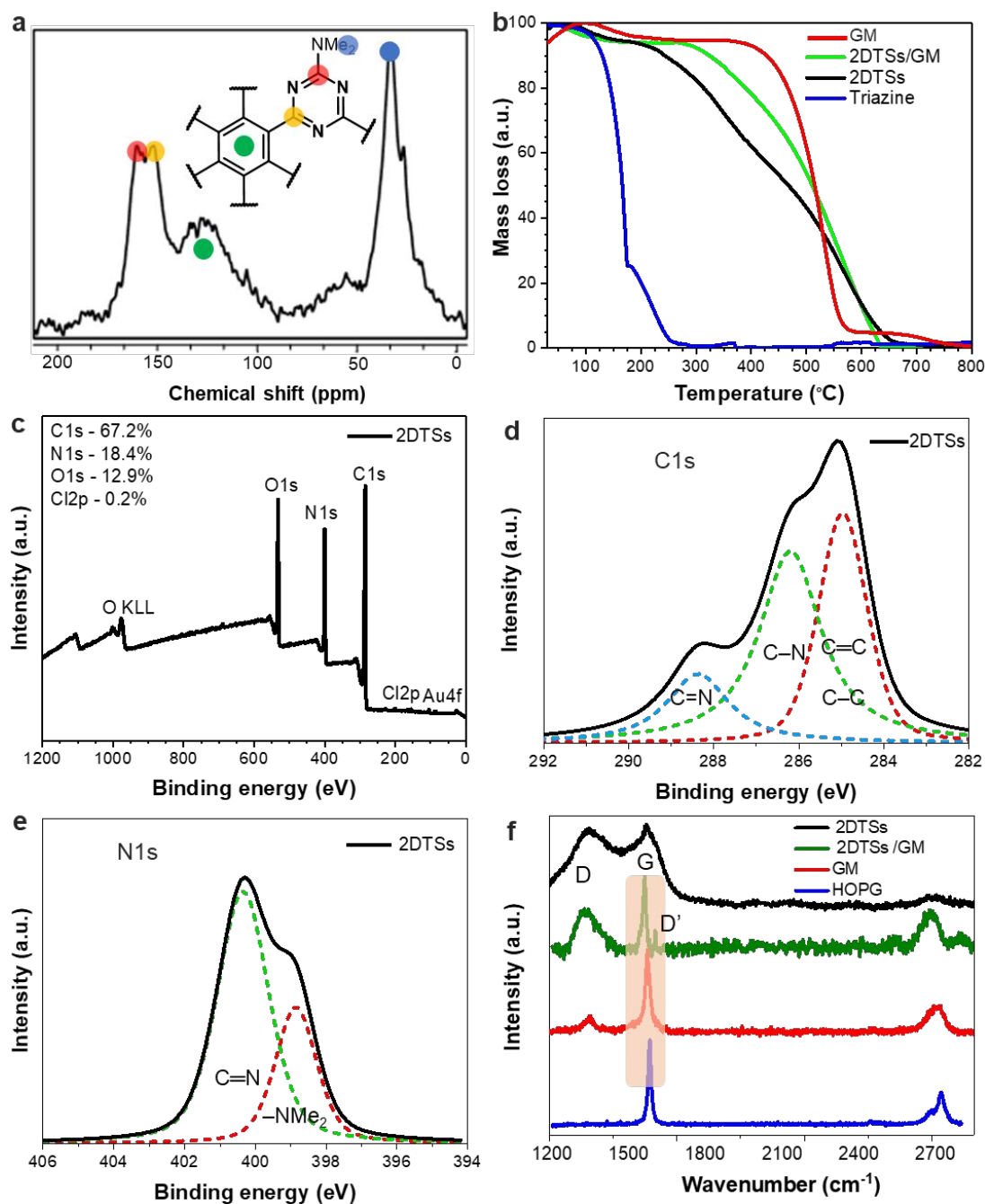


Figure 3. Characterization of 2DTSSs by spectroscopy methods and thermal analysis. **(a)** ^{13}C CP-MAS-NMR spectrum of 2DTSSs showed distinguished signals for the triazine and benzene rings as well as $-\text{NMe}_2$ functional groups. **(b)** TGA thermograms of 2DTSSs, cyanuric chloride GM, and GM/2DTSSs. **(c)** Survey XPS spectrum of 2DTSSs with quantification table of the main elements. Absence of the calcium peak after washing process confirmed the successful removal of metal ions. Au4f peak originates from the substrate. **(d)** Highly resolved XPS C1s spectrum and **(e)** highly resolved XPS N1s spectrum of 2DTSSs. Fit parameters for each spectrum and interpretations are shown in table S2. **(f)** A close up of

1
2
3 Raman spectra overlay of the G peak and D' peak regions of the 2DTSSs, GM, and highly
4 oriented pyrolytic graphite (HOPG).
5
6
7

8 The thermal behavior of 2DTSSs was investigated by thermogravimetric analysis
9 (TGA) in air. Their thermal stability correlated with the nitrogen content of the products.
10 Materials with lower nitrogen contents, which are the products of reactions in aqueous
11 solution or non-anhydrous condition, showed higher thermal stability. This is an indicator for
12 the higher graphitic content of these materials. Based on literature reports, the reaction
13 between water and calcium carbide is the source of graphitic materials in our reactions.⁵³
14 While the production of GM occurs at room temperature, the reaction between calcium
15 carbide and cyanuric chloride requires temperatures around 120 °C. Therefore, the production
16 of GM is kinetically favored, and cyanuric chloride does not play a role at low temperatures.
17 In the TGA thermogram of 2DTSSs, weight losses in low and high temperature ranges are
18 assigned to the detachment of $-NMe_2$ functional groups and decomposition of the backbone of
19 this nanomaterial, respectively (Figure 3b). The structure of 2DTSSs was further investigated
20 by X-ray photoelectron spectroscopy (XPS). Carbon, nitrogen, as the main components, and
21 oxygen were detected in the survey spectrum of 2DTSSs (Figure 3c). The highly resolved C1s
22 XPS spectrum (Figure 3d) showed three intense C1s component peaks at 288.4 eV,
23 representing carbon atoms of triazine rings,⁵⁹ and at 286.2 and 285.0 eV, corresponding to the
24 $-NMe_2$ groups and carbons of benzene rings, respectively.^{54, 58, 60} Two components in the N1s
25 peak at 400.4 eV and 398.9 eV were assigned to the nitrogen atoms of triazine rings and $-$
26 NMe_2 groups, respectively (Figure 3e).^{58, 61} The absence of the calcium peak in the survey
27 spectrum of 2DTSSs is a proof of the successful removal of calcium upon purification (Figure
28 3c).
29
30
31
32
33
34
35
36
37
38
39
40
41
42
43
44

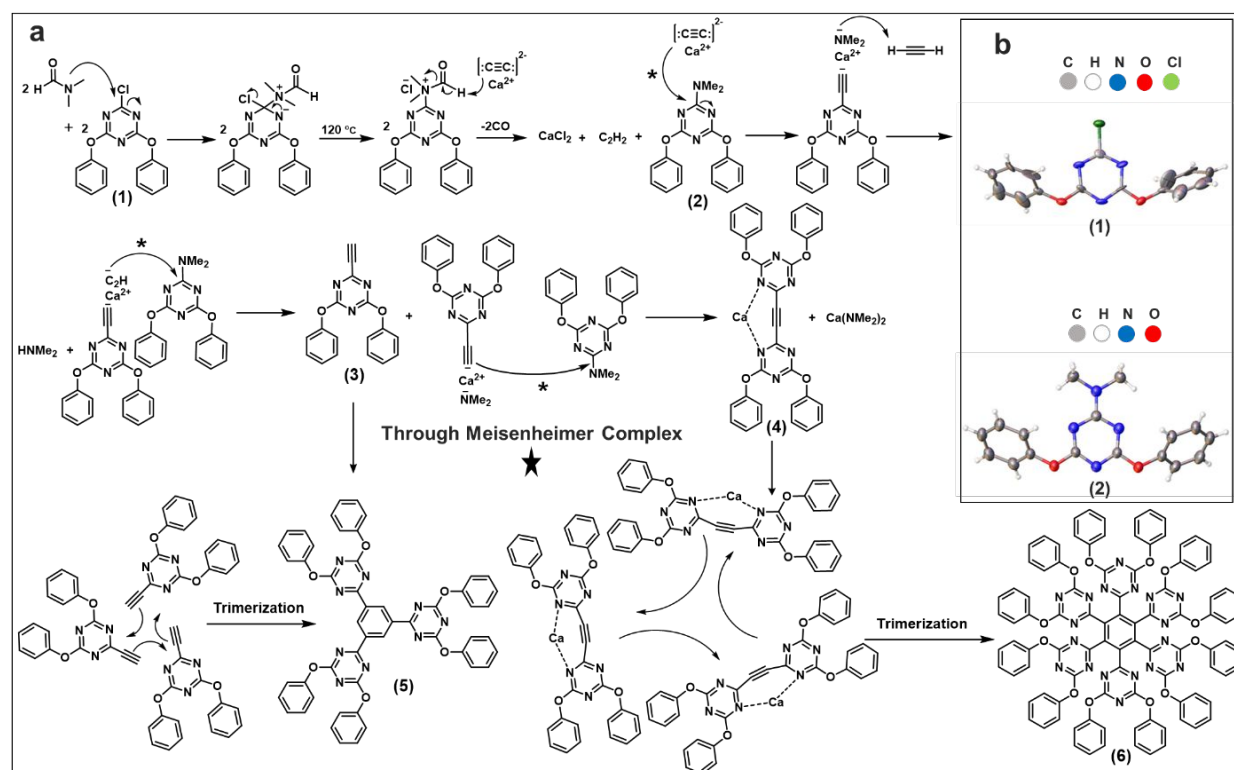
45 In order to complement the characterization of the synthesized materials through
46 investigation of their polymorphism and crystallinity, their Raman spectra were individually
47 evaluated and mapped (Figures 3f and S7). The G peaks of 2DTSSs and GM were appeared at
48 1562 cm^{-1} and 1582 cm^{-1} , respectively. In the case of 2DTSSs, broadening of Raman peaks at
49 $1320\text{--}1360\text{ cm}^{-1}$ area, centered at 1345 cm^{-1} , as well as peaks at $1550\text{--}1620\text{ cm}^{-1}$ area with a
50 pronounced peak at $1562\text{ to }1565\text{ cm}^{-1}$ was observed. As it is previously reported by Ferrari et
51 al.,⁶² the C=N vibrational frequencies are very similar to the C=C within the $1000\text{ to }2000\text{ cm}^{-1}$
52 range. Therefore, the observed peaks in the Raman spectra of 2DTSSs were assigned to a
53 structure with the embedded nitrogen atoms. Furthermore, increasing the nitrogen content of
54 products affected the G peak position in their Raman spectra, when visible laser light was
55
56
57
58
59
60

1
2
3 used. For example, for a product with 20-30% nitrogen content, a G peak at 1560-1565 cm^{-1}
4 was observed which is in agreement with the reported data in literature.⁶² This downshift in
5 comparison with the G peak of HOPG was assigned to the difference between GM
6 composition and HOPG.⁶² The direct correlation between this shift and the nitrogen content of
7 the materials is a further proof for the preparation of 2DTSs at anhydrous conditions.
8 Furthermore, 2DTSs/GM mixtures exhibit Raman bands at $\sim 1332 \text{ cm}^{-1}$ and $\sim 1564 \text{ cm}^{-1}$ with
9 an occasional weak and broad band at $\sim 1610\text{-}1620 \text{ cm}^{-1}$ in addition to a broad band centered
10 at $\sim 2700 \text{ cm}^{-1}$ (Figure 3f). The Raman bands at $\sim 1345 \text{ cm}^{-1}$ and $\sim 1620 \text{ cm}^{-1}$, which
11 correspond to the D peak, are assigned to the domain boundaries or nucleation sites within the
12 structure. On the other hand, the D' peak observed occasionally at $\sim 1620 \text{ cm}^{-1}$ demonstrates
13 the doping by a hetero atom, suggesting nitrogen atoms of triazine in the structure of 2DTSs
14 (Figure 3f). It is important to note that no band at $\sim 2100 \text{ cm}^{-1}$ was observed in the spectrum
15 of 2DTSs. In agreement with IR and NMR spectra, this is a further proof of the trimerization
16 of triple bonds.⁶³⁻⁶⁴

17
18
19
20
21
22
23
24
25
26
27
28
29
30
31
32
33
34
35
36
37
38
39
40
41
42
43
44
45
46
47
48
49
50
51
52
53
54
55
56
57
58
59
60
After analyzing the chemical structure of the two-dimensional structures, the
mechanism of their synthetic pathway and structures of intermediates were investigated. To
avoid polymerization and to constrain the reaction to the molecular level, two active sites of
cyanuric chloride were blocked by phenol, and 2-chloro-4,6-diphenoxy-1,3,5-s-triazine (**1**)
was synthesized according to reported methods in literature⁶⁵ (see Figures S8-11 for NMR
and mass spectra). Then the reaction between 2-chloro-4,6-diphenoxy-1,3,5-s-triazine and
calcium carbide was carried out in anhydrous DMF at 120 °C. Different characterization
methods showed that the chlorine atom of 2-chloro-4,6-diphenoxy-1,3,5-s-triazine was
substituted by DMF leading to 2-(*N,N*-dimethylamino)-4,6-diphenoxy-s-triazine (**2**) (Figure
4a). The structure of compound (**2**) was investigated by single X-ray crystallography and
spectroscopy methods (Figure 4b-d). ¹H-NMR showed a chemical shift for the phenoxy
protons of compound (**1**) after reaction with DMF. Also, a signal for -NMe₂ protons appeared
in the spectrum of compound (**2**) (Figure 4c). Comparison of ¹³C NMR spectra of compounds
(**1**) and (**2**) showed a distinct C-Cl chemical shift from 173.8 ppm to 167.4 ppm after reaction
with DMF. These results were in agreement with literature⁶⁶⁻⁶⁷ and confirmed substitution of
the chlorine atom of compound (**1**) by -NMe₂ groups, which were derived from DMF (Figure
4d). The structure of intermediate (**2**) was further proven by mass spectrometry. The signals at
309.1 and 331.1 m/z are related to the molar mass of this compound accompanied by proton
and sodium ion, respectively (calculated for C₁₇H₁₆N₄O₂ [M+H] and [M+Na]: 309.1 and
331.1, respectively, Figure S11). Accordingly, the signal of methyl groups in the CP-MAS-

1
2
3 NMR of 2DTSs can be assigned to $-NMe_2$ groups that are created by reaction between DMF
4 and cyanuric chloride. Reaction between compound (**2**) and calcium carbide resulted in
5 compounds (**3** and **4**). This reaction was monitored at intervals of two hours by Matrix-
6 Assisted Laser Desorption/Ionization Time-of-Flight (MALDI-TOF) and electrospray
7 ionization mass spectrometry (ESI) for three days. Signal at 328.11 m/z and 655.25 m/z
8 (Figures S12 and S13) are assigned to compounds **3** and **4**, which were converted to
9 compounds **5** and **6**, respectively upon trimerization. Compound **4** was accompanied by one
10 or two calcium ions (Figures S13 and S14), which showed that metal-ligand interactions were
11 possible driving forces to inhibit rotation of triazine rings around linkages and direct
12 polymerization in two dimensions. However, compound **4**, which was accompanied by one
13 calcium ion, could be more reactive toward trimerization, due to less steric hindrance.
14 Compounds **5** and **6** were detected by MALDI-TOF (Figure 4e). These compounds proved
15 formation of benzene rings in the structure of 2DTSs upon trimerization of triple bonds.
16 Furthermore, fragments at 336 m/z and 639 m/z in the ESI mass spectrum of this model
17 reaction indicated building blocks consisting benzene rings with six substituents (Figures S14
18 and S15). This result showed that calcium carbide can react with triazine rings from both
19 sides because trimerization of the product of such a reaction results in a 2D polymer
20 consisting of benzene rings with six substituents. It is worth noting that in compound **6**
21 triazine rings were able to rotate to minimize the repulsion of electron pair of adjacent
22 nitrogen atoms. However, in 2DTSs rotation of such units is restricted leading to an
23 energetically unfavorable structure. Therefore, the units created by di-substituted calcium
24 carbide can be mostly at the edges or defect sites, where the electron repulsion of adjacent
25 nitrogen atoms is reduced. The backbone of 2DTSs consist mostly of graphitic domains or
26 regions created by trimerization of mono-substituted calcium carbide or a mixture with its di-
27 substituted analog (Figure 1b). In addition to MALDI-TOF spectra, 1H NMR indicated the
28 formation of mono-substituted calcium carbide. 1H NMR of the product of reaction between
29 2-chloro-4,6-diphenoxy-1,3,5-s-triazine and calcium carbide showed clear signals for
30 compounds **5**, which could be created by trimerization of mono-substituted calcium carbide
31 (Figure S16). The reaction mechanism was further investigated by synthesizing 2,4-dichloro-
32 6-phenoxy-1,3,5-s-triazine and polymerization of this monomer in DMF under the same
33 reaction conditions (Scheme S1). In the MALDI-TOF spectrum of the product of this
34 reaction, distinguished peaks at $243n$ m/z intervals, where n is a natural number, indicated a
35 repeating unit with benzene substituents (Figure S17). This repeating unit is a further proof of
36 the nucleophilic substitution of chlorine atoms of triazine followed by trimerization. The role
37
38
39
40
41
42
43
44
45
46
47
48
49
50
51
52
53
54
55
56
57
58
59
60

of DMF in the reaction between cyanuric chloride and calcium carbide was further proven by changing the solvent to N,N-dimethylacetamide, toluene, and mesitylene. Accomplishment of reaction in these solvents did not result in any detectable product. This experiment proved the critical role of DMF in the production of two-dimensional triazine structure. As indicated by compound (3), complexation of intermediates with calcium ions hampered the rotation of triazine rings around acetylide linkages and directed the consequent reactions in two dimensions (Figure S18). The directing role of calcium ions was further investigated by DFT functional in GPAW program⁶⁸⁻⁷⁰ (see page S23 and S24).



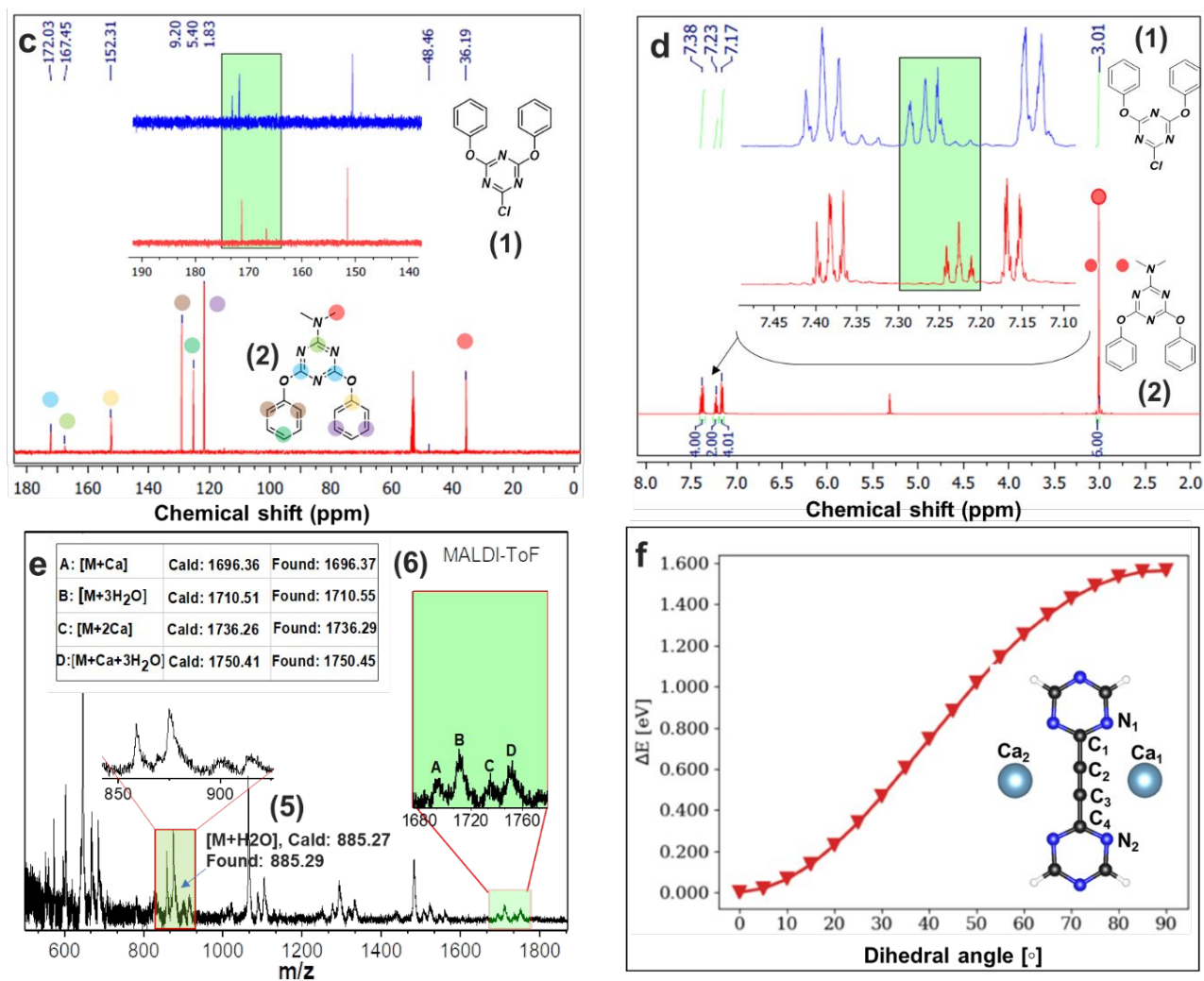


Figure 4. Investigation of the mechanism of the reaction between cyanuric chloride and calcium carbide in DMF using model compounds. (a) Reaction between compound (1) and DMF resulted in intermediate (2). Consequently, nucleophilic reaction between compound (2) and calcium carbide resulted in compounds 3 and 4 that converted to compounds 5 and 6 upon trimerization. (b) Single crystal XRD structure of compounds (1) and (2). (c) and (d) ^{13}C - and ^1H -NMR spectra of compound (1) and compound (2), respectively. (e) Expanded MALDI-TOF spectrum of mixture of reaction between compound 1 and cyanuric chloride in DMF. (f) The simulated structure of model compound coordinated with two calcium ions (on both sides) and the total energy of the system with different dihedral angle with step size of 5° (see details in Figure S18 and Table S3).

Coordination of one or two calcium ions with nitrogen atoms of the triazine rings in compound 4 (phenyl groups were replaced by hydrogen) caused 0.05 eV and 1.6 eV barrier energy, respectively, for rotation around C₁-C₂ and C₃-C₄ and bonds (Figure 4f). These energy barriers are driving forces for growing triazine-benzene structures in two dimensions.

According to the literature, calcium ions are able to form complexes with nitrogen containing ligands such as 1,10-phenanthroline, 4,4'-bipyridine and 2,2'-bipyridine.⁷¹⁻⁷² While interactions between these ligands and calcium ions are not as strong as oxygen containing ligands,⁷³⁻⁷⁴ they are able to induce enough rigidity for the two-dimensional coupling of monomers.⁶⁸⁻⁷⁰ The weakness of the interactions on the other hand enables that the metal ions can be removed completely from the final product. Another proof of the directing role of calcium ions was achieved by adding sodium carbonate to the reaction medium. When the reaction between cyanuric chloride and calcium carbide was performed in DMF and in the presence of sodium carbonate, no sheet-like structure was achieved, due to the production of sodium carbonate and absence of any driving force to conjugate monomers in a sheet-like structure (Figure S19).

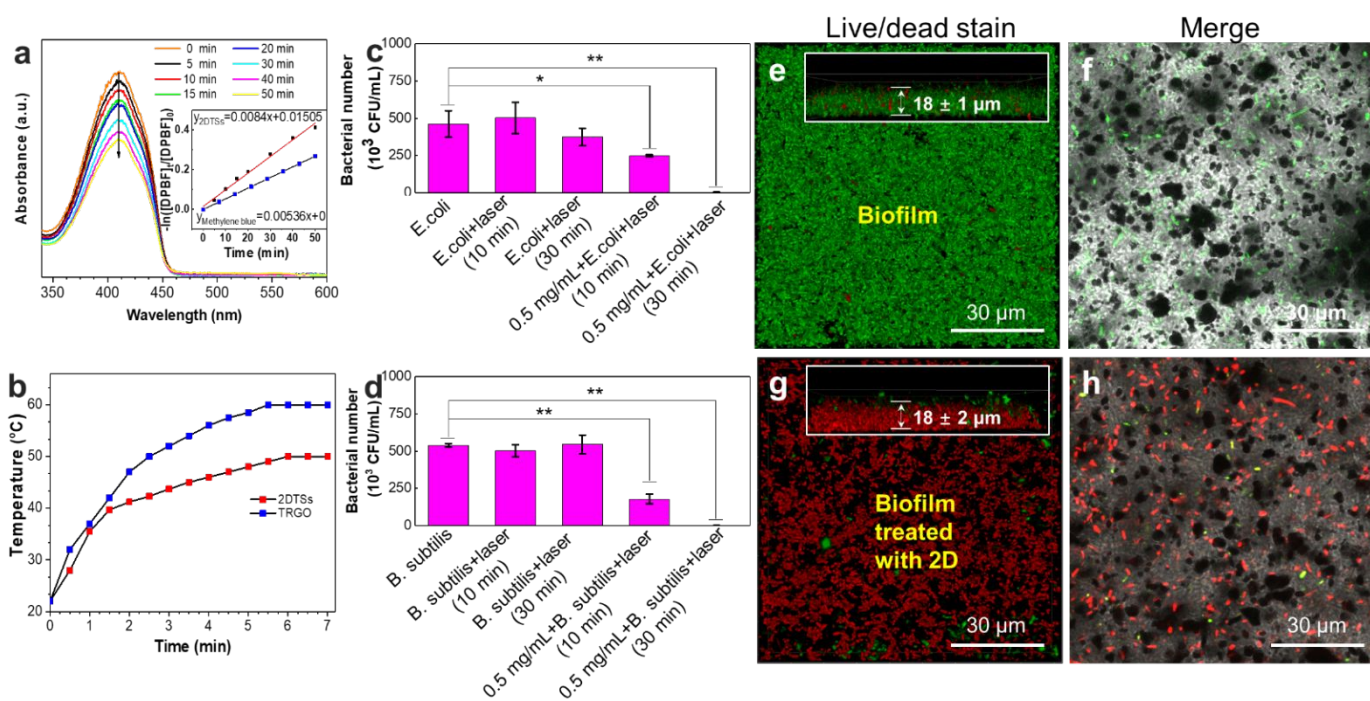


Figure 5. (a) Singlet oxygen generation kinetics of water dispersion of 2DTSSs and (b) photothermal properties of 2DTSSs under laser irradiation (808 nm, 0.5 W/cm²). Thermally reduced graphene oxide (TRGO) was used as control, the concentration was 0.5 mg/mL in water (more details can be found in page S27). (c) and (d) antibacterial activities of samples (0.5 mg/mL) against *E. coli* and *B. subtilis*. *E. coli* and *B. subtilis* in PBS were used as controls. Data are presented as mean ± SD, n = 3. Statistically significant differences are indicated by *p < 0.05 and **p < 0.01 compared with the control. (e-h) biofilm eradication test: the bacteria entrapped in biofilm were destroyed by 2DTSSs upon laser irradiation. In

1
2
3 live/dead assay, live and dead bacteria are shown by green and red colors respectively (details
4 are available in page S27).
5
6

7
8 The photochemical properties of 2DTSs were investigated by different methods.
9 2DTSs showed a maximum UV absorption at 235-276 nm corresponding to $n \rightarrow \pi^*$ transitions
10 (Figure S20). Due to their large π -conjugated system, 2DTSs were able to produce singlet
11 oxygen under irradiation with near infrared (NIR) laser (808 nm). This was confirmed using
12 1,3-Diphenylisobenzofuran (DPBF) as a specific singlet oxygen scavenger (Figure 5a).
13 2DTSs demonstrated a higher singlet oxygen production rate as observed by absorbance
14 change of DPBF in comparison to methylene blue as a photosensitizer reference in similar
15 solvent. This property could be used for different applications ranging from photodynamic
16 therapy to photocatalyst applications. Laser irradiation of a water dispersion of 2DTSs
17 elevated the medium temperature from 20 °C to 40 °C in 2 minutes (Figure 5b). The
18 production of heat is less efficient than by thermally reduced graphene oxide but still in a
19 suitable range for some applications including photothermal therapy or antibacterial activity.
20 Accordingly, the antibacterial activity of 2DTSs under laser irradiation was investigated.
21 While laser irradiation did not show a significant adverse effect against bacteria, 2DTSs (0.5
22 mg/mL) followed by 10 minutes laser irradiation resulted in incapacitation of 46% and 67%
23 *E.coli* and *B. subtilis* respectively (Figures 5c,d). Prolongation of the laser irradiation to 30
24 min resulted in destruction of both gram positive and gram negative bacteria completely (in
25 the detection limit). The bacteria entrapped in biofilm are more resistant to biocide, due to
26 protection and sufficient nutrition inside the biofilm. Therefore, antibiofilm property of an
27 antibacterial agent is of high relevance and determines its efficiency for the treatment of
28 contaminated surfaces. Incubation of 2DTSs with an 18 μm thick biofilm for 1 h followed by
29 laser irradiation for 30 min resulted in destruction of bacteria inside the biofilm, proven by red
30 fluorescence (Figures 5e, g). As Figures 5f and 5h show, 2DTSs with black color penetrated
31 into the biofilm and incapacitated bacteria (more details in page S27).
32
33
34
35
36
37
38
39
40
41
42
43
44
45
46
47
48

49 Our results showed that the reaction between calcium carbide and triazine in DMF is
50 an efficient strategy to develop versatile two-dimensional triazine structures through the
51 concepts of reticular chemistry. Deep understanding of the mechanism of this reaction can
52 help us to manipulate the structure of the products by changing reaction parameters including
53 precursors, metal ion, solvent, and water content.
54
55
56
57
58
59
60

CONCLUSION

The reaction between cyanuric chloride and calcium carbide under anhydrous conditions was mediated by *N, N*-dimethylformamide to produce 2D triazine-benzene structures on the gram scale. A mechanistic study revealed a dual role of the calcium carbide, first as a source of acetylide ions, which created benzene rings upon trimerization, and second the calcium ions could act as a two-dimensional directing force upon interaction with triazine rings. Adding water showed a high impact on the reaction route and in the presence of water, graphitic material was created. Taking advantage of its interesting physicochemical properties, straightforward synthesis and cheap precursors, the presented two-dimensional nanomaterial is a promising candidate for a wide range of future applications including photodynamic and photothermal therapy.

ASSOCIATED CONTENT

Supporting Information

Experimental details; SEM, TEM, HRTEM and SFM images; EELS spectra and PXRD diffractograms; IR, Raman & NMR spectra; Mass spectrometry; XPS interpretation; computational analysis (DFT calculation).

AUTHOR INFORMATION

Corresponding Authors

Arne Thomas – *Department of Chemistry / Functional Materials, Technische Universität Berlin, Hardenbergstraße 40, 10623 Berlin, Germany; Email: arne.thomas@tu-berlin.de*

Mohsen Adeli – *Institut für Chemie und Biochemie, Freie Universität Berlin, Arnimallee 22, Berlin 14195, Germany. Faculty of Science, Department of Chemistry, Lorestan University, Khorramabad, Iran; Email: m.aadeli@fu-berlin.de*

Authors

Abbas Faghani – *Institut für Chemie und Biochemie, Freie Universität Berlin, Arnimallee 22, Berlin 14195, Germany*

Mohammad Fardin Gholami – *Department of Physics & IRIS Adlershof, Humboldt-Universität zu Berlin, Newtonstr. 15, 12489 Berlin Germany*

Matthias Trunk – *Department of Chemistry / Functional Materials, Technische Universität Berlin, Hardenbergstraße 40, 10623 Berlin, Germany*

Johannes Müller – *Department of Physics & IRIS Adlershof, Humboldt-Universität zu Berlin, Newtonstr. 15, 12489 Berlin Germany*

1
2
3 **Pradip Pachfule** – *Department of Chemistry / Functional Materials, Technische Universität*
4 *Berlin, Hardenbergstraße 40, 10623 Berlin, Germany*

5
6 **Sarah Vogl** – *Department of Chemistry / Functional Materials, Technische Universität*
7 *Berlin, Hardenbergstraße 40, 10623 Berlin, Germany*

8
9
10 **Ievgen Donskyi** – *Institut für Chemie und Biochemie, Freie Universität Berlin, Arnimallee*
11 *22, Berlin 14195, Germany. BAM – Federal Institute for Material Science and Testing,*
12 *Division of Surface Analysis and Interfacial Chemistry, Unter den Eichen 44-46, 12205*
13 *Berlin, Germany*

14
15
16
17 **Mingjun Li** – *Institut für Chemie und Biochemie, Freie Universität Berlin, Arnimallee 22,*
18 *Berlin 14195, Germany. Center for Health Science and Engineering, Tianjin Key Laboratory*
19 *of Materials Laminating Fabrication and Interface Control Technology, School of Materials*
20 *Science and Engineering, Hebei University of Technology, Tianjin 300130, China*

21
22
23
24 **Philip Nickl** – *Institut für Chemie und Biochemie, Freie Universität Berlin, Arnimallee 22,*
25 *Berlin 14195, Germany. BAM – Federal Institute for Material Science and Testing, Division*
26 *of Surface Analysis and Interfacial Chemistry, Unter den Eichen 44-46, 12205 Berlin,*
27 *Germany*

28
29
30
31 **Jingjing Shao** – *Institut für Chemie und Biochemie, Freie Universität Berlin, Arnimallee 22,*
32 *Berlin 14195, Germany*

33
34 **Michael Huang** – *Department of Physics & IRIS Adlershof, Humboldt-Universität zu Berlin,*
35 *Newtonstr. 15, 12489 Berlin Germany*

36
37
38 **Wolfgang E. S. Unger** – *BAM – Federal Institute for Material Science and Testing, Division*
39 *of Surface Analysis and Interfacial Chemistry, Unter den Eichen 44-46, 12205 Berlin,*
40 *Germany*

41
42
43 **Raul Arenal** – *Laboratorio de Microscopias Avanzadas (LMA), Instituto de Nanociencia de*
44 *Aragon, Universidad de Zaragoza, 50018 Zaragoza, Spain. Fundacion ARAID, 50018*
45 *Zaragoza, Spain. Instituto de Ciencias de Materiales de Aragon, CSIC-Universidad de*
46 *Zaragoza, 50009 Zaragoza, Spain*

47
48
49
50 **Christoph T. Koch** – *Department of Physics & IRIS Adlershof, Humboldt-Universität zu*
51 *Berlin, Newtonstr. 15, 12489 Berlin Germany*

52
53
54 **Beate Paulus** – *Institut für Chemie und Biochemie, Freie Universität Berlin, Arnimallee 22,*
55 *Berlin 14195, Germany*

56
57
58 **Jürgen P. Rabe** – *Department of Physics & IRIS Adlershof, Humboldt-Universität zu Berlin,*
59 *Newtonstr. 15, 12489 Berlin Germany*

Rainer Haag – *Institut für Chemie und Biochemie, Freie Universität Berlin, Arnimallee 22, Berlin 14195, Germany*

ACKNOWLEDGMENTS

We thank the German Science Foundation (DFG) for financial support within the grants SFB 765 and SFB 658. M.F.G. and J.P.R. also acknowledge the support of the Cluster of Excellence “Matters of Activity. Image Space Material” funded by the DFG under Germany’s Excellence Strategy EXC 2025. Furthermore, A.T. acknowledges the DFG for funding within the project TH 1463/12-1. We would like to thank Dr. Andreas Schäfer and Maiko Schulze for solid-NMR experiments as well as we appreciate the effort of Vahid Ahmadi Soureshjani for MALDI-TOF experiments. We would like to acknowledge M. Eng. Jörg M. Stockmann for operating the XPS instrument at the BAM, Prof. Stephanie Reich and Dr. Antonio Setaro for fruitful discussions. 2DTs-HRTEM and -EELS studies were conducted at the Laboratorio de Microscopias Avanzadas, Instituto de Nanociencia de Aragon, Universidad de Zaragoza, Spain. R.A. gratefully acknowledges the support from the Spanish Ministry of Economy and Competitiveness (MINECO) through project grant MAT2016-79776-P (AEI/FEDER, UE) and from the European Union H2020 programs ETN projects “Graphene Flagship” (785219) and “ESTEEM3” (823717).

REFERENCES

1. Pei, W.-Y.; Xu, G.; Yang, J.; Wu, H.; Chen, B.; Zhou, W.; Ma, J.-F., Versatile Assembly of Metal-Coordinated Calix[4]resorcinarene Cavitands and Cages through Ancillary Linker Tuning. *J. Am. Chem. Soc.* **2017**, *139* (22), 7648-7656.
2. Ma, T.; Kapustin, E. A.; Yin, S. X.; Liang, L.; Zhou, Z.; Niu, J.; Li, L.-H.; Wang, Y.; Su, J.; Li, J.; Wang, X.; Wang, W. D.; Wang, W.; Sun, J.; Yaghi, O. M., Single-crystal x-ray diffraction structures of covalent organic frameworks. *Science* **2018**, *361* (6397), 48-52.
3. Diercks, C. S.; Liu, Y.; Cordova, K. E.; Yaghi, O. M., The role of reticular chemistry in the design of CO₂ reduction catalysts. *Nat. Mater.* **2018**, *17* (4), 301-307.
4. Feng, L.; Wang, K.-Y.; Lv, X.-L.; Yan, T.-H.; Li, J.-R.; Zhou, H.-C., Modular Total Synthesis in Reticular Chemistry. *J. Am. Chem. Soc.* **2020**, *142* (6), 3069-3076.
5. Payamyar, P.; King, B. T.; Öttinger, H. C.; Schlüter, A. D., Two-dimensional polymers: concepts and perspectives. *ChemComm* **2016**, *52* (1), 18-34.
6. Baumann, A. E.; Burns, D. A.; Liu, B.; Thoi, V. S., Metal-organic framework functionalization and design strategies for advanced electrochemical energy storage devices. *Commun. Chem.* **2019**, *2* (1), 86.
7. Geng, K.; He, T.; Liu, R.; Dalapati, S.; Tan, K. T.; Li, Z.; Tao, S.; Gong, Y.; Jiang, Q.; Jiang, D., Covalent Organic Frameworks: Design, Synthesis, and Functions. *Chem. Rev.* **2020**.
8. Molina, M.; Asadian-Birjand, M.; Balach, J.; Bergueiro, J.; Miceli, E.; Calderón, M., Stimuli-responsive nanogel composites and their application in nanomedicine. *Chem. Soc. Rev.* **2015**, *44* (17), 6161-6186.

9. Xu, F.; Yang, S.; Chen, X.; Liu, Q.; Li, H.; Wang, H.; Wei, B.; Jiang, D., Energy-storage covalent organic frameworks: improving performance via engineering polysulfide chains on walls. *Chem. Sci.* **2019**, *10* (23), 6001-6006.
10. Yuan, S.; Li, X.; Zhu, J.; Zhang, G.; Van Puyvelde, P.; Van der Bruggen, B., Covalent organic frameworks for membrane separation. *Chem. Soc. Rev.* **2019**, *48* (10), 2665-2681.
11. Côté, A. P.; Benin, A. I.; Ockwig, N. W.; O'Keeffe, M.; Matzger, A. J.; Yaghi, O. M., Porous, Crystalline, Covalent Organic Frameworks. *Science* **2005**, *310* (5751), 1166-1170.
12. Montoro, C.; Rodríguez-San-Miguel, D.; Polo, E.; Escudero-Cid, R.; Ruiz-González, M. L.; Navarro, J. A. R.; Ocón, P.; Zamora, F., Ionic Conductivity and Potential Application for Fuel Cell of a Modified Imine-Based Covalent Organic Framework. *J. Am. Chem. Soc.* **2017**, *139* (29), 10079-10086.
13. Zhang, J.; Han, X.; Wu, X.; Liu, Y.; Cui, Y., Multivariate Chiral Covalent Organic Frameworks with Controlled Crystallinity and Stability for Asymmetric Catalysis. *J. Am. Chem. Soc.* **2017**, *139* (24), 8277-8285.
14. Evans, A. M.; Parent, L. R.; Flanders, N. C.; Bisbey, R. P.; Vitaku, E.; Kirschner, M. S.; Schaller, R. D.; Chen, L. X.; Gianneschi, N. C.; Dichtel, W. R., Seeded growth of single-crystal two-dimensional covalent organic frameworks. *Science* **2018**, *361* (6397), 52-57.
15. Liu, M.; Huang, Q.; Wang, S.; Li, Z.; Li, B.; Jin, S.; Tan, B., Crystalline Covalent Triazine Frameworks by In Situ Oxidation of Alcohols to Aldehyde Monomers. *Angew. Chem. Int. Ed.* **2018**, *57* (37), 11968-11972.
16. Kuhn, P.; Antonietti, M.; Thomas, A., Porous, Covalent Triazine-Based Frameworks Prepared by Ionothermal Synthesis. *Angew. Chem. Int. Ed.* **2008**, *47* (18), 3450-3453.
17. Algara-Siller, G.; Severin, N.; Chong, S. Y.; Björkman, T.; Palgrave, R. G.; Laybourn, A.; Antonietti, M.; Khimyak, Y. Z.; Krasheninnikov, A. V.; Rabe, J. P.; Kaiser, U.; Cooper, A. I.; Thomas, A.; Bojdys, M. J., Triazine-Based Graphitic Carbon Nitride: a Two-Dimensional Semiconductor. *Angew. Chem. Int. Ed.* **2014**, *53* (29), 7450-7455.
18. Guo, X.; Tian, Y.; Zhang, M.; Li, Y.; Wen, R.; Li, X.; Li, X.; Xue, Y.; Ma, L.; Xia, C.; Li, S., Mechanistic Insight into Hydrogen-Bond-Controlled Crystallinity and Adsorption Property of Covalent Organic Frameworks from Flexible Building Blocks. *Chem. Mater.* **2018**, *30* (7), 2299-2308.
19. Liu, M.; Guo, L.; Jin, S.; Tan, B., Covalent triazine frameworks: synthesis and applications. *J. Mater. Chem. A* **2019**, *7* (10), 5153-5172.
20. Noda, Y.; Merschjann, C.; Tarábek, J.; Amsalem, P.; Koch, N.; Bojdys, M. J., Directional Charge Transport in Layered Two-Dimensional Triazine-Based Graphitic Carbon Nitride. *Angew. Chem. Int. Ed.* **2019**, *58* (28), 9394-9398.
21. Tuci, G.; Pilaski, M.; Ba, H.; Rossin, A.; Luconi, L.; Caporali, S.; Pham-Huu, C.; Palkovits, R.; Giambastiani, G., Unraveling Surface Basicity and Bulk Morphology Relationship on Covalent Triazine Frameworks with Unique Catalytic and Gas Adsorption Properties. *Adv. Funct. Mater.* **2017**, *27* (7), 1605672.
22. Zhu, H.; Lin, W.; Li, Q.; Hu, Y.; Guo, S.; Wang, C.; Yan, F., Bipyridinium-Based Ionic Covalent Triazine Frameworks for CO₂, SO₂, and NO Capture. *ACS Appl. Mater. Interfaces* **2020**, *12* (7), 8614-8621.
23. Lee, Y. J.; Talapaneni, S. N.; Coskun, A., Chemically Activated Covalent Triazine Frameworks with Enhanced Textural Properties for High Capacity Gas Storage. *ACS Appl. Mater. Interfaces* **2017**, *9* (36), 30679-30685.
24. Yang, K.; Yuan, W.; Hua, Z.; Tang, Y.; Yin, F.; Xia, D., Triazine-Based Two-Dimensional Organic Polymer for Selective NO₂ Sensing with Excellent Performance. *ACS Appl. Mater. Interfaces* **2020**, *12* (3), 3919-3927.
25. El-Mahdy, A. F. M.; Kuo, C.-H.; Alshehri, A.; Young, C.; Yamauchi, Y.; Kim, J.; Kuo, S.-W., Strategic design of triphenylamine- and triphenyltriazine-based two-dimensional covalent organic frameworks for CO₂ uptake and energy storage. *J. Mater. Chem. A* **2018**, *6* (40), 19532-19541.
26. Roeser, J.; Kailasam, K.; Thomas, A., Covalent Triazine Frameworks as Heterogeneous Catalysts for the Synthesis of Cyclic and Linear Carbonates from Carbon Dioxide and Epoxides. *ChemSusChem* **2012**, *5* (9), 1793-1799.

- 1
2
3 27. Lan, Z.-A.; Fang, Y.; Zhang, Y.; Wang, X., Photocatalytic Oxygen Evolution from Functional
4 Triazine-Based Polymers with Tunable Band Structures. *Angew. Chem. Int. Ed.* **2018**, *57* (2), 470-474.
- 5 28. Guo, L.; Niu, Y.; Razzaque, S.; Tan, B.; Jin, S., Design of D–A1–A2 Covalent Triazine
6 Frameworks via Copolymerization for Photocatalytic Hydrogen Evolution. *ACS Catalysis* **2019**, *9* (10),
7 9438-9445.
- 8 29. Artz, J., Covalent Triazine-based Frameworks—Tailor-made Catalysts and Catalyst Supports
9 for Molecular and Nanoparticulate Species. *ChemCatChem* **2018**, *10* (8), 1753-1771.
- 10 30. Li, Y.; Zheng, S.; Liu, X.; Li, P.; Sun, L.; Yang, R.; Wang, S.; Wu, Z.-S.; Bao, X.; Deng, W.-Q.,
11 Conductive Microporous Covalent Triazine-Based Framework for High-Performance Electrochemical
12 Capacitive Energy Storage. *Angew. Chem. Int. Ed.* **2018**, *57* (27), 7992-7996.
- 13 31. Vadiyar, M. M.; Liu, X.; Ye, Z., Macromolecular Polyethynylbenzotrile Precursor-Based
14 Porous Covalent Triazine Frameworks for Superior High-Rate High-Energy Supercapacitors. *ACS Appl.*
15 *Mater. Interfaces* **2019**, *11* (49), 45805-45817.
- 16 32. Hao, L.; Ning, J.; Luo, B.; Wang, B.; Zhang, Y.; Tang, Z.; Yang, J.; Thomas, A.; Zhi, L., Structural
17 Evolution of 2D Microporous Covalent Triazine-Based Framework toward the Study of High-
18 Performance Supercapacitors. *J. Am. Chem. Soc.* **2015**, *137* (1), 219-225.
- 19 33. Tan, C.; Cao, X.; Wu, X.-J.; He, Q.; Yang, J.; Zhang, X.; Chen, J.; Zhao, W.; Han, S.; Nam, G.-H.;
20 Sindoro, M.; Zhang, H., Recent Advances in Ultrathin Two-Dimensional Nanomaterials. *Chem. Rev.*
21 **2017**, *117* (9), 6225-6331.
- 22 34. Bojdys, M. J.; Jeromenok, J.; Thomas, A.; Antonietti, M., Rational Extension of the Family of
23 Layered, Covalent, Triazine-Based Frameworks with Regular Porosity. *Adv. Mater.* **2010**, *22* (19),
24 2202-2205.
- 25 35. Wang, K.; Yang, L.-M.; Wang, X.; Guo, L.; Cheng, G.; Zhang, C.; Jin, S.; Tan, B.; Cooper, A.,
26 Covalent Triazine Frameworks via a Low-Temperature Polycondensation Approach. *Angew. Chem.*
27 *Int. Ed.* **2017**, *56* (45), 14149-14153.
- 28 36. Ren, S.; Bojdys, M. J.; Dawson, R.; Laybourn, A.; Khimyak, Y. Z.; Adams, D. J.; Cooper, A. I.,
29 Porous, Fluorescent, Covalent Triazine-Based Frameworks Via Room-Temperature and Microwave-
30 Assisted Synthesis. *Adv. Mater.* **2012**, *24* (17), 2357-2361.
- 31 37. Troschke, E.; Grätz, S.; Lübken, T.; Borchardt, L., Mechanochemical Friedel–Crafts
32 Alkylation—A Sustainable Pathway Towards Porous Organic Polymers. *Angew. Chem. Int. Ed.* **2017**,
33 *56* (24), 6859-6863.
- 34 38. Liu, J.; Zan, W.; Li, K.; Yang, Y.; Bu, F.; Xu, Y., Solution Synthesis of Semiconducting Two-
35 Dimensional Polymer via Trimerization of Carbonitrile. *J. Am. Chem. Soc.* **2017**, *139* (34), 11666-
36 11669.
- 37 39. Liu, J.; Lyu, P.; Zhang, Y.; Nachtigall, P.; Xu, Y., New Layered Triazine Framework/Exfoliated 2D
38 Polymer with Superior Sodium-Storage Properties. *Adv. Mater.* **2018**, *30* (11), 1705401.
- 39 40. Yu, S.-Y.; Mahmood, J.; Noh, H.-J.; Seo, J.-M.; Jung, S.-M.; Shin, S.-H.; Im, Y.-K.; Jeon, I.-Y.;
40 Baek, J.-B., Direct Synthesis of a Covalent Triazine-Based Framework from Aromatic Amides. *Angew.*
41 *Chem. Int. Ed.* **2018**, *57* (28), 8438-8442.
- 42 41. Lyu, H.; Diercks, C. S.; Zhu, C.; Yaghi, O. M., Porous Crystalline Olefin-Linked Covalent Organic
43 Frameworks. *J. Am. Chem. Soc.* **2019**, *141* (17), 6848-6852.
- 44 42. Acharjya, A.; Pachfule, P.; Roeser, J.; Schmitt, F.-J.; Thomas, A., Vinylene-Linked Covalent
45 Organic Frameworks by Base-Catalyzed Aldol Condensation. *Angew. Chem. Int. Ed.* **2019**, *58* (42),
46 14865-14870.
- 47 43. Jiang, X.; Wang, P.; Zhao, J., 2D covalent triazine framework: a new class of organic
48 photocatalyst for water splitting. *J. Mater. Chem. A* **2015**, *3* (15), 7750-7758.
- 49 44. Jin, H.; Guo, C.; Liu, X.; Liu, J.; Vasileff, A.; Jiao, Y.; Zheng, Y.; Qiao, S.-Z., Emerging Two-
50 Dimensional Nanomaterials for Electrocatalysis. *Chem. Rev.* **2018**, *118* (13), 6337-6408.
- 51 45. Ball, B.; Chakravarty, C.; Sarkar, P., Two-Dimensional Covalent Triazine Framework as a
52 Promising Anode Material for Li-Ion Batteries. *J. Phys. Chem. C* **2019**, *123* (50), 30155-30164.
- 53 46. Venkanna, P.; Rajanna, K. C.; Satish Kumar, M.; Bismillah Ansari, M.; Moazzam Ali, M., 2,4,6-
54 Trichloro-1,3,5-triazine and N,N'-dimethylformamide as an effective Vilsmeier–Haack reagent for the
55
56
57
58
59
60

- 1
2
3 synthesis of 2-chloro-3-formyl quinolines from acetanilides. *Tetrahedron Lett.* **2015**, *56* (37), 5164-
4 5167.
- 5 47. Scott, M. D.; Spedding, H., Vilsmeier adducts of dimethylformamide. *J. Chem. Soc. C* **1968**,
6 (0), 1603-1609.
- 7 48. De Luca, L.; Giacomelli, G.; Porcheddu, A., An Efficient Route to Alkyl Chlorides from Alcohols
8 Using the Complex TCT/DMF. *Org. Lett.* **2002**, *4* (4), 553-555.
- 9 49. Arenal, R.; March, K.; Ewels, C. P.; Rocquefelte, X.; Kociak, M.; Loiseau, A.; Stéphan, O.,
10 Atomic Configuration of Nitrogen-Doped Single-Walled Carbon Nanotubes. *Nano Lett.* **2014**, *14* (10),
11 5509-5516.
- 12 50. Ayala, P.; Arenal, R.; Rummeli, M.; Rubio, A.; Pichler, T., The doping of carbon nanotubes with
13 nitrogen and their potential applications. *Carbon* **2010**, *48* (3), 575-586.
- 14 51. Arenal, R.; De Matteis, L.; Custardoy, L.; Mayoral, A.; Tence, M.; Grazu, V.; De La Fuente, J.
15 M.; Marquina, C.; Ibarra, M. R., Spatially-Resolved EELS Analysis of Antibody Distribution on
16 Biofunctionalized Magnetic Nanoparticles. *ACS Nano* **2013**, *7* (5), 4006-4013.
- 17 52. Ayala, P.; Arenal, R.; Loiseau, A.; Rubio, A.; Pichler, T., The physical and chemical properties of
18 heteronanotubes. *Rev. Mod. Phys.* **2010**, *82* (2), 1843-1885.
- 19 53. Jia, Y.; Chen, X.; Zhang, G.; Wang, L.; Hu, C.; Sun, X., Topotactic conversion of calcium carbide
20 to highly crystalline few-layer graphene in water. *J. Mater. Chem. A* **2018**, *6* (46), 23638-23643.
- 21 54. Casco, M. E.; Kirshhoff, S.; Leistenschneider, D.; Rauche, M.; Brunner, E.; Borchardt, L.,
22 Mechanochemical synthesis of N-doped porous carbon at room temperature. *Nanoscale* **2019**, *11*
23 (11), 4712-4718.
- 24 55. Chen, X.; Zhang, L.; Zhao, Y.; Wang, X.; Ke, C., Graphene folding on flat substrates. *J. Appl.*
25 *Phys.* **2014**, *116* (16), 164301.
- 26 56. Gholami, M. F.; Severin, N.; Rabe, J. P., Folding of Graphene and Other Two-dimensional
27 Materials. In *On Folding: Towards a New Field of Interdisciplinary Research*, M. Friedmann, W. S., Ed.
28 transcript: 2016; pp 211-237.
- 29 57. Chen, Y.; Wang, X., Template-Free Synthesis of Hollow G-C₃N₄ Polymer with Vesicle
30 Structure for Enhanced Photocatalytic Water Splitting. *J. Phys. Chem.* **2018**, *122* (7), 3786-3793.
- 31 58. Xiang, Z.; Cao, D.; Huang, L.; Shui, J.; Wang, M.; Dai, L., Nitrogen-Doped Holey Graphitic
32 Carbon from 2D Covalent Organic Polymers for Oxygen Reduction. *Adv. Mater.* **2014**, *26* (20), 3315-
33 3320.
- 34 59. Tahir, M.; Mahmood, N.; Zhu, J.; Mahmood, A.; Butt, F. K.; Rizwan, S.; Aslam, I.; Tanveer, M.;
35 Idrees, F.; Shakir, I.; Cao, C.; Hou, Y., One Dimensional Graphitic Carbon Nitrides as Effective Metal-
36 Free Oxygen Reduction Catalysts. *Sci. Rep.* **2015**, *5* (1), 12389.
- 37 60. Chen, W.; Huang, L.; Yi, X.; Zheng, A., Lithium doping on 2D squaraine-bridged covalent
38 organic polymers for enhancing adsorption properties: a theoretical study. *PCCP* **2018**, *20* (9), 6487-
39 6499.
- 40 61. Faghani, A.; Donskyi, I. S.; Fardin Gholami, M.; Ziem, B.; Lippitz, A.; Unger, W. E. S.; Böttcher,
41 C.; Rabe, J. P.; Haag, R.; Adeli, M., Controlled Covalent Functionalization of Thermally Reduced
42 Graphene Oxide To Generate Defined Bifunctional 2D Nanomaterials. *Angew. Chem. Int. Ed.* **2017**, *56*
43 (10), 2675-2679.
- 44 62. Ferrari, A. C.; Robertson, J.; Ferrari, A. C.; Robertson, J., Raman spectroscopy of amorphous,
45 nanostructured, diamond-like carbon, and nanodiamond. *PHILOS T R SOC A* **2004**, *362* (1824), 2477-
46 2512.
- 47 63. Cataldo, F., The role of Raman spectroscopy in the research on sp-hybridized carbon chains:
48 carbynoid structures polyynes and metal polyynides. *J RAMAN SPECTROSC* **2008**, *39* (2), 169-176.
- 49 64. Wang, J.; Zhang, S.; Zhou, J.; Liu, R.; Du, R.; Xu, H.; Liu, Z.; Zhang, J.; Liu, Z., Identifying sp-sp₂
50 carbon materials by Raman and infrared spectroscopies. *PCCP* **2014**, *16* (23), 11303-11309.
- 51 65. Namazi, H.; Adeli, M., Solution proprieties of dendritic triazine/poly(ethylene
52 glycol)/dendritic triazine block copolymers. *J. Polym. Sci., Part A: Polym. Chem.* **2005**, *43* (1), 28-41.
- 53 66. Agarwal, A.; Chauhan, P. M. S., Convenient Dimethylamino Amination in Heterocycles and
54 Aromatics with Dimethylformamide. *Synth. Commun.* **2004**, *34* (16), 2925-2930.
- 55
56
57
58
59
60

- 1
2
3 67. Heravi, Majid M.; Ghavidel, M.; Mohammadkhani, L., Beyond a solvent: triple roles of
4 dimethylformamide in organic chemistry. *RSC Adv.* **2018**, *8* (49), 27832-27862.
5 68. Mortensen, J. J.; Hansen, L. B.; Jacobsen, K. W., Real-space grid implementation of the
6 projector augmented wave method. *Phys. Rev. B* **2005**, *71* (3), 035109.
7 69. Enkovaara, J.; Rostgaard, C.; Mortensen, J. J.; Chen, J.; Duřak, M.; Ferrighi, L.; Gavnholt, J.;
8 Glinsvad, C.; Haikola, V.; Hansen, H. A.; Kristoffersen, H. H.; Kuisma, M.; Larsen, A. H.; Lehtovaara, L.;
9 Ljungberg, M.; Lopez-Acevedo, O.; Moses, P. G.; Ojanen, J.; Olsen, T.; Petzold, V.; Romero, N. A.;
10 Stausholm-Møller, J.; Strange, M.; Tritsarlis, G. A.; Vanin, M.; Walter, M.; Hammer, B.; Häkkinen, H.;
11 Madsen, G. K. H.; Nieminen, R. M.; Nørskov, J. K.; Puska, M.; Rantala, T. T.; Schiøtz, J.; Thygesen, K. S.;
12 Jacobsen, K. W., Electronic structure calculations with GPAW: a real-space implementation of the
13 projector augmented-wave method. *J. Phys.: Condens. Matter* **2010**, *22* (25), 253202.
14 70. Marques, M. A. L.; Oliveira, M. J. T.; Burnus, T., Libxc: A library of exchange and correlation
15 functionals for density functional theory. *Comput. Phys. Commun.* **2012**, *183* (10), 2272-2281.
16 71. Ghasemi, J.; Shamsipur, M., Fluorimetric Study of Complexation of Alkali and Alkaline Earth
17 Cations with 1,10-Phenanthroline, 2,2'-Bipyridine and 8-Hydroxyquinoline in Nonaqueous Solvents. *J.*
18 *Coord. Chem.* **1992**, *26* (4), 337-344.
19 72. Murugavel, R.; Korah, R., Structural Diversity and Supramolecular Aggregation in Calcium,
20 Strontium, and Barium Salicylates Incorporating 1,10-Phenanthroline and 4,4'-Bipyridine: Probing
21 the Softer Side of Group 2 Metal Ions with Pyridinic Ligands. *Inorg. Chem.* **2007**, *46* (26), 11048-
22 11062.
23 73. Mitchell, P. R.; Sigel, H., Ternary complexes in solution. Enhanced stability of ternary metal
24 ion/adenosine 5'-triphosphate complexes. Cooperative effects caused by stacking interactions in
25 complexes containing adenosine triphosphate, phenanthroline, and magnesium, calcium, or zinc
26 ions. *J. Am. Chem. Soc.* **1978**, *100* (5), 1564-1570.
27 74. Noro, S.-i.; Mizutani, J.; Hijikata, Y.; Matsuda, R.; Sato, H.; Kitagawa, S.; Sugimoto, K.;
28 Inubushi, Y.; Kubo, K.; Nakamura, T., Porous coordination polymers with ubiquitous and
29 biocompatible metals and a neutral bridging ligand. *Nat. Commun.* **2015**, *6* (1), 5851.
30
31
32
33
34
35
36
37
38
39
40
41
42
43
44
45
46
47
48
49
50
51
52
53
54
55
56
57
58
59
60

1
2
3 For Table of Contents Only
4
5
6
7
8
9
10
11
12
13
14
15
16
17
18
19
20
21
22
23
24
25
26
27
28
29
30
31
32
33
34
35
36
37
38
39
40
41
42
43
44
45
46
47
48
49
50
51
52
53
54
55
56
57
58
59
60

